Stochastic approach to plastic deformation of polymers

Masroor, S.

Award date:
2013

Stochastic Approach to Plastic Deformation of Polymers

Saeed Masroor

August 2013

Eindhoven University of Technology

Master's theses

Stochastic Approach to Plastic Deformation of Polymers

Author:
Saeed Masroor

Supervisor:
Prof. M.A. Peletier
Dr. M. Hütter

A thesis submitted in fulfilment of the requirements
for the degree of Master of Science in Industrial and Applied Mathematics

in the

Center of Analysis, Scientific Computing and Applications
Department of Mathematics and Computer Science

August 2013

EINDHOVEN UNIVERSIRT OF TECHNOLOGY

Abstract

Department of Mathematics and Computer Science

Master of Science in Industrial and Applied Mathematics

Stochastic Approach to Plastic Deformation of Polymers

by Saeed Masroor

Behind the plastic deformation in polymers lies a thermally activated process. This process consists of breakage of (inter-molecular) bonds and slippage of polymer chains on each other. The well-known Eyring model provides a heuristic picture of transition from elastic to plastic regime. In this thesis a stochastic version of the Eyring model is constructed in order to improve the classical model. The volume of the sample under deformation comes into play and affects the amplitude of the noise. Then a particle systems approach is proposed as a possible way of treating the problem. Possible challenges are discussed as well as the need for a more rigorous understanding of the process since one observes large fluctuation of the noise near the yield point. In this respect, a toy model has been constructed as a discrete analogue of plastic deformation. For this model numerical simulations are given and continuum limits are taken to finally obtain a stochastic differential equation. The stochastic Eyring model and the limit of the discrete system are compared and it is emphasized that the stochastic description of the system in terms of Fokker-Planck equation or the corresponding stochastic differential equation is valid only in small amplitude noise regime.

Acknowledgements

Special thanks go to Mark Peletier for providing excellent support, advice, and encouragement. I would like to thank Markus Hütter for the beautiful problem he proposed. Working with him on this problem helped me overcome the fear of working with stochastic processes.

I would like to thank the Assessment Committee, Dr. Jan ten Thije Boonkkamp, for reading my thesis and also for his great course on Scientific Computing in PDEs. I also learned very much from the courses given by Dr Sorin Pop and Dr. Adrean Muntean; hereby I want to express my appreciation to them.

Many friends have helped me during the past two years and making my life productive and enjoyable. I am lucky to have made such great friends. Without their endless appreciation for food my cooking skills would not have improved this much.

My parents receive the deepest gratitude and love for the many years of support.

I am extremely happy that TU/e has given me the opportunity to continue my research for another four years.

Contents

List of Figures

List of Tables

Dedicated to

Aidin Bozorgi, Pouya Keivan, and Mojtaba Jarahi
who reached the summit of mount Broad Peak via a new route.
They will forever remain in the Himalayas, and in our hearts and minds. May their souls rest in peace.

Chapter 1

Introduction

1.1 Plastic deformation

Deformation of solids in the plastic regime is very important in engineering sciences. Understanding the behaviour of materials during plastic flow helps engineers to control this process and produce new products. In this thesis, the material of interest is polycarbonate (PC), a widely used polymer. PC is ductile (i.e. it can withstand significant strains before rupture). A typical stress-strain graph for PC is demonstrated in Figure (1.1). Under homogeneous deformation first a linear relation between stress and strain

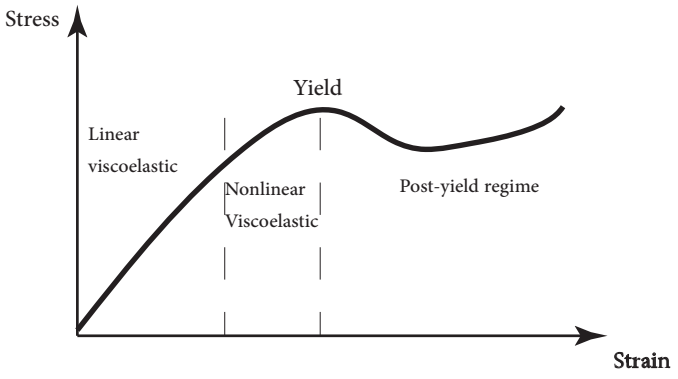

FIGURE 1.1: Schematic stress-strain curve for Polycarbonate.

is observed. Then the material shows a nonlinear response plastic deformation occurs. After that one observes strain-softening and strain-hardening before rupture. As the interest of this study is the transition from elastic regime to the yield point, a brief explanation of underlying molecular mechanisms will follow.

1.2 The rate theory of plastic deformation

Within the structure of a polymer material, chains are hold together by inter-molecular and intra-molecular bonds. The origin of deformation in polymers is the breakage and establishment of intra-molecular bonds. Even in the absence of stress, like any material thermal energy in the system gives rise to molecular mobility i.e. molecules break inter-molecular bonds and change their conformation [1]. A first study of kinetics of materials in fracture and flow was done by *Henry Eyring* [2]. As a result of his studies it became known that plastic deformation of polymers is a thermally activated process. Thermally activated processes are events whose occurrence are passages between different stable configurations of the system that are separated by free energy barriers and the frequency of jumps depends strongly on temperature. This frequency, ν, is given by

$$\nu = \nu_0 \exp(-\frac{\Delta E}{kT}) \tag{1.1}$$

where ν_0 is a constant, ΔE is the height of the energy barrier called *activation energy*, k is the Boltzmann constant, and T is the temperature.
In the absence of stress, the jumps over the energy barrier occur rarely but in a statistically balanced manner. Eyring [2],p6, showed that when a stress field, σ, is applied

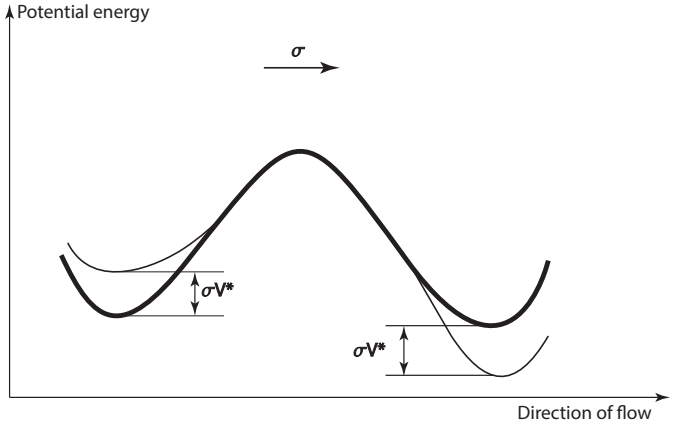

FIGURE 1.2: The effect of applied stress on the energy barrier. A bundle of molecules go from one equilibrium to another one. The thick line is the energy landscape in the absence of applied flow and the thin line in the presence of applied flow.

to a polymer, the frequency of jumping forward (ν_f) and backward (ν_b) over the energy barrier changes to

$$\nu_f = \nu_0 \exp(-\frac{\Delta E - \sigma V^*}{kT}) \tag{1.2}$$

$$\nu_b = \nu_0 \exp(-\frac{\Delta E + \sigma V^*}{kT}). \tag{1.3}$$

where V^* is called *activation volume* and is a characteristic volume associated to the entangled network of polymer chains. A flow unit i.e., a polymer chain or a bundle of chains, sweeps a certain volume as it slips. The imposed stress multiplied by activation volume has the units of energy and Eyring associated this energy to the energy barrier that has to be surmounted in the flow process [3] [2]p,38. This theory is based on the assumption that shear transformation is highly localized and only involves a few segments. Moreover the plastic strain rate is proportional to the net rate of the flow over the barrier.

$$\begin{aligned} \dot{\gamma}_p &\propto (\nu_f - \nu_b) \\ &= 2\nu_0 \exp\left(-\frac{\Delta E}{kT}\right) \sinh\left(\frac{\sigma V^*}{kT}\right) \end{aligned}$$

This means that for the plastic strain rate $\dot{\gamma}_p$ one can write

$$\dot{\gamma}_p = \dot{\gamma}_0 \exp(-\frac{\Delta E}{kT}) \sinh(\frac{\sigma}{\sigma_0}) \tag{1.4}$$

where $\dot{\gamma}_0$ is a proportionality constant and $\sigma_0 = kT/V^*$ is a characteristic volume.

1.3 Objective of the thesis

The classical Eyring model for plastic deformation results in a stress-strain curve which has considerable differences with the actual curve obtained by experiment, see Figure 1.3. The objective of this thesis is to find out whether randomness of the underlying molecular events is responsible for this mismatch between the result of Eyring model and result of the experiments. In this respect the plan is to obtain a stochastic version of Eyring model for plastic deformation of polymers and see whether adding noise has an observable macroscopic effect. In particular we are interested to see whether the sharp kink in the transition from elastic to plastic regime can be smoothed by adding noise to the problem. In addition to this, understanding the connection between different models

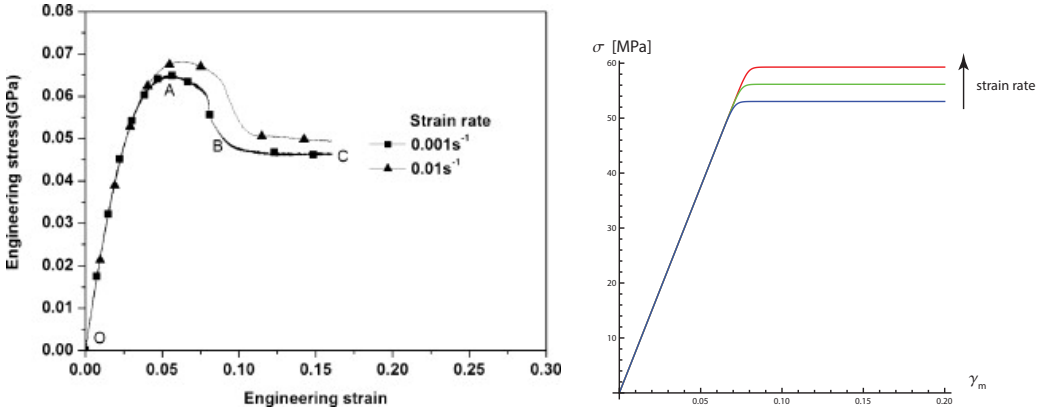

FIGURE 1.3: Results of experiment of tensile test (left)taken from [7] and the result from Eyring model (right)

is also part of the plan.

1.4 Outline of the thesis

This thesis is organized as follows: In chapter 2 after introducing the concepts involved in kinetic theory of deformation of polymers, the Eyring model is derived. Then it is made clear how the parameters of the model are obtained from experiment. Then noting the drawbacks of the Eyring model, a stochastic differential equation is derived and shown to model the plastic deformation. In this respect certain important assumptions are made. The resulting SDE is solved by an adaptive Euler-Maruyama scheme and the results are discussed.

In chapter 3 it is motivated that how the process of plastic deformation can be viewed as an interacting system of particles (polymer blocks). Then the framework of a particle systems approach to the problem is established and possible challenges are discussed.

Observing the need for a more rigorous understanding of the Eyring model, a toy model

is constructed in chapter 4 which describes a discrete analogue of the thermally activated process of plastic flow. This new model is studied numerically and then the continuum limit of this discrete system is taken utilizing Kramers-Moyal expansion. Then obtaining a Fokker-Planck equation allows writing down an SDE. At the end this model is compared to the stochastic Eyring model from chapter 2 and the results are discussed in chapter 5.

Chapter 2

From Deterministic to Stochastic Eyring Model

2.1 Formulation of the ODE

2.1.1 Eyring model for shear deformation

The mechanism of shear deformation is illustrated in Figure 2.1. For the sake of simplicity the model is restricted to plane deformation. An important assumption in this

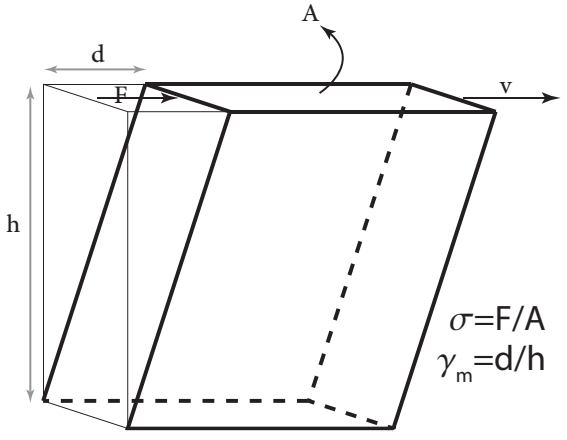

FIGURE 2.1: Mechanism of shear deformation: σ is the shear stress, A is the area, F the force applied, v the velocity of imposed deformation, and γ_m the corresponding "macroscopic" shear strain. The strain rate is $\dot{\gamma}_m = \frac{v}{h}$.

study is that the imposed strain, γ_m, consists of two parts: the elastic component, γ_e, and the plastic component, γ_p.

$$\gamma_m = \gamma_e + \gamma_p \tag{2.1}$$

This assumption is equivalent to a model consisting of an Eyring dashpot series with an elastic element which results in splitting of deformation into two components [5],p236. It was shown in chapter 1 that the plastic strain rate is stress dependent:

$$\dot{\gamma}_p \quad = \quad \dot{\gamma}_0 \exp(-\frac{\Delta E}{kT}) \sinh(\frac{\sigma}{\sigma_0}).$$

Suppose that the test in Figure 2.1 is performed on a polymer e.g. polycarbonate. Initially the stress is low and causes only small change in plastic strain rate. Continued imposed strain increases the stress and thus the plastic strain rate $\dot{\gamma}_p$ until eventually it becomes equal to the total applied strain rate $\dot{\gamma}_m$. At this point the polymer stops elastic stretching i.e. $\dot{\gamma}_e = 0$ at yield point. This mechanism produces a behaviour that resembles yield.

In order to formulate the visco-plastic behaviour of polymers, it is common to introduce the so called Eyring viscosity [4]. It is a stress dependent viscosity

$$\eta(\sigma) := \eta_0 \frac{\frac{\sigma}{\sigma_0}}{\sinh\left(\frac{\sigma}{\sigma_0}\right)} \tag{2.2}$$

where the *zero viscosity* is

$$\eta_0 = \frac{\sigma_0}{\dot{\gamma}_0} \exp\left(\frac{\Delta E}{RT}\right). \tag{2.3}$$

Now it is easy to see that the expression for $\dot{\gamma}_p$ can be written as

$$\dot{\gamma}_p = \frac{\sigma}{\eta(\sigma)} \tag{2.4}$$

Moreover let $\Phi(\gamma_e(t))$ be the strain energy density (elastic energy per volume) of the system. Then the stress can be obtained by the following relation.

$$\sigma = \frac{\partial \Phi(\gamma_e)}{\partial \gamma_e} \tag{2.5}$$

A typical choice for Φ is

$$\Phi(\gamma_e) = \frac{1}{2}\, G\, \gamma_e^2 \tag{2.6}$$

which is used throughout the thesis. Here G is the shear modulus i.e. $\sigma = G\gamma_e$

Taking a time derivative of equation (2.1) and using relation (1.4) for plastic strain rate and equation (2.5) for stress, lead to a general form of the Eyring model:

$$\dot{\gamma_e}(t) = \dot{\gamma}_m - \frac{1}{\eta} \frac{\partial \Phi(\gamma_e)}{\partial \gamma_e}. \tag{2.7}$$

2.1.2 Parameters

It was previously discussed that at yield point $\dot{\gamma}_m = \dot{\gamma}_p$. Also because the yield stress, σ_Y, is larger than σ_0, one can make use of the approximation

$$\sinh\left(\frac{\sigma_Y}{\sigma_0}\right) \approx \frac{1}{2}\exp\left(\frac{\sigma_Y}{\sigma_0}\right) \tag{2.8}$$

to obtain the yield stress predicted by Eyring model:

$$\begin{aligned}\sigma_Y &= \frac{kT}{V^*}\ln\left(\frac{2\dot{\gamma}_m}{\dot{\gamma}_0}\exp\left(\frac{\Delta E}{kT}\right)\right) \\ &= \frac{kT}{V^*}\left(\ln(\dot{\gamma}_m) + \ln\left(\frac{2}{\dot{\gamma}_0}\exp(\frac{\Delta E}{kT})\right)\right)\end{aligned} \tag{2.9}$$

Figure 2.2 from [5] is the result of many tensile tests. The yield stress over temperature is plotted as a function of the logarithm of imposed strain rate. At a fixed temperature the slope is determined by the activation volume and it is seen the data can be nicely interpolated by sets of parallel straight lines meaning that V^* is obtained by a good accuracy. The three unknown parameters are reported in [6] and [1] and are presented

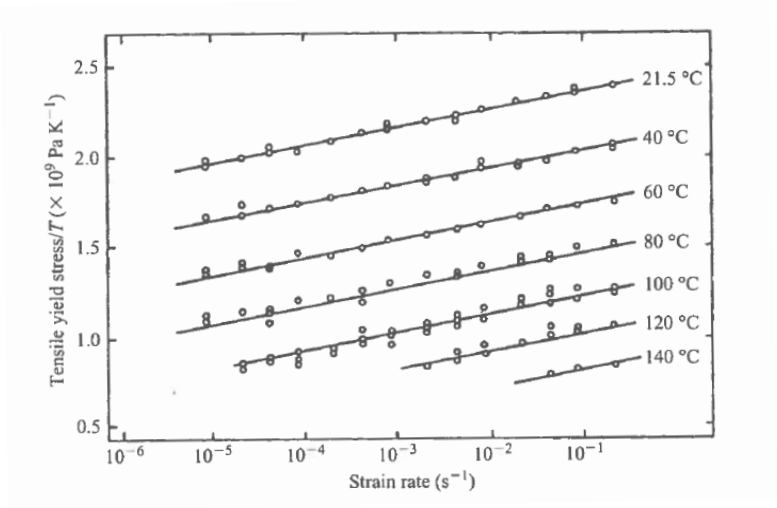

FIGURE 2.2: Measured ratio of yield stress to temperature as a function of the logarithm of imposed strain rate for polycarbonate. Taken from [5] p,239

in table (2.1).

$\dot{\gamma}_0$	$1.118 \times 10^{27} s^{-1}$
V^*	$3.05 \times 10^{-27} m^3$
$\Delta U = N_A \Delta E$	274 kJ/mol

TABLE 2.1: Eyring parameters for polycarbonate Lexan 161R. Taken from [1]

2.2 How good is the Eyring model?

Setting $\gamma_e(0) = 0$ and letting $\dot{\gamma}_m$ be constant, one can obtain a numerical solution of equation 2.7 for different values of imposed strain rate. Figure 2.3 shows these solutions. It is observed the plateau value of stress is an increasing function of $\dot{\gamma}_m$ which can be seen also from equation (2.9).

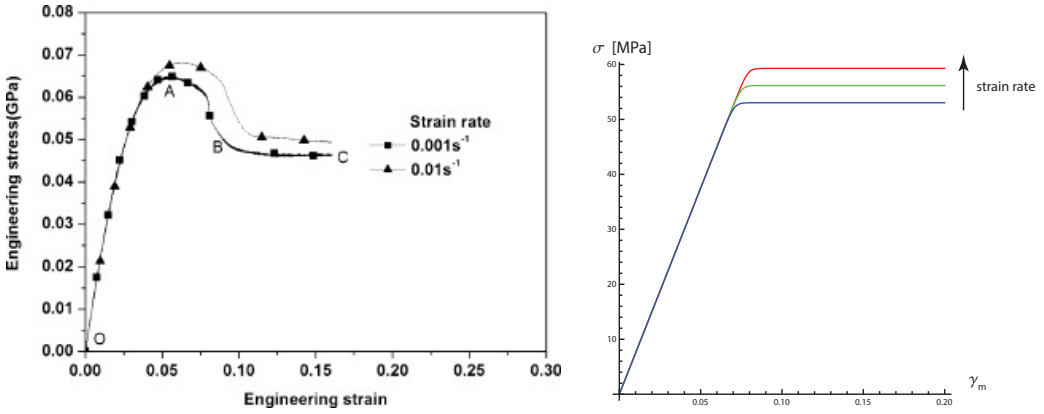

FIGURE 2.3: Results of experiment of tensile test (left) taken from [1] and the result from Eyring model (right) for different constant imposed strain rates. $10^{-4}s^{-1}$ (blue), $10^{-3}s^{-1}$ (green), $10^{-2}s^{-1}$ (red)

Comparison of the deterministic solution to experimental data, shows that the transition to yield in the Eyring model is very sharp, as seen in Figure 2.3 and that is not similar to what is observed in experiment. See Figure 2.3 (left) which is taken from reference [7]. This sharp transition to yield is the main difference of the model and experimental data. This sharp kink in the stress-strain curve resulted from Eyring model can be smoothed if σ_0 becomes larger, or equivalently saying, V^* becomes smaller. However in view of the discussion in previous section, there is strong evidence that the activation volume is fixed and obtained by a good accuracy. Therefore there are other reasons for this mismatch.

At micro level, the processes involved in plastic deformation are of statistical nature. The Eyring model provides a heuristic picture of these micro effects. If the volume of the sample under shear is small enough, then due to change of the configuration of polymer chains at micro level, the randomness of the process shows its effect and one expects to see fluctuations in the corresponding stress-strain curve. In the Eyring model there is no sample volume involved. This observation suggests the idea that it might be possible to obtain a stochastic version of the Eyring model which can show the effect of fluctuations.

2.3 Formulation of the SDE

In [8] a toy model has been constructed to obtain a stochastic description of the dynamics of sliding layers representative of plastic deformation of single crystalline metals. Inspired by their approach, a similar construction will be established here for polymer chains. In order to construct a stochastic version of Eyring model, it is assumed that equation (2.7) is perturbed by a (thermal) noise, i.e. the evolution of γ_e can be described by the following stochastic differential equation

$$d\gamma_e = \left(\dot{\gamma}_m + A - \frac{1}{\eta}\frac{\partial \Phi}{\partial \gamma_e}\right) dt + \sqrt{2D} dW_t. \tag{2.10}$$

The prefactor $\sqrt{2D}$ in the noise term represents the strength of fluctuations, with dW_t as the random increment of a stochastic Wiener process with statistical averages $< dW_t >= 0$ and $< dW_t, dW_t' >= \delta(t-t')dt$. The need for adding this additional term A will be explained soon. The corresponding Fokker-Planck equation ,[9] p.111, describing the evolution of probability density $p(\gamma_e, t)$ is as follows.

$$\frac{\partial p}{\partial t} = -\frac{\partial}{\partial \gamma_e}\left(\left[\dot{\gamma}_m + \left(A - \frac{1}{\eta}\frac{\partial \Phi}{\partial \gamma_e}\right)\right] p\right) + \frac{\partial}{\partial \gamma_e}\frac{\partial}{\partial \gamma_e}(Dp) \tag{2.11}$$

In order to find A and D, it is postulated that the equilibrium distribution of the Fokker-Planck equation in the absence of applied flow is of the form

$$p_{eq} = \frac{1}{Z}\exp\left(-\frac{\Phi\Omega}{kT}\right) \tag{2.12}$$

where Ω is the volume of the sample under shear deformation and Z is a normalization factor and can be obtained using the fact that $\int_{-\infty}^{+\infty} p_{eq}\, d\gamma_e = 1$.
In the absence of applied flow, i.e. $\dot{\gamma}_m = 0$, substitution of the equilibrium distribution in the Fokker-Planck equation 2.11 gives

$$\begin{aligned}
-\frac{\partial}{\partial \gamma_e}\left(\left[\left(A - \frac{1}{\eta}\frac{\partial \Phi}{\partial \gamma_e}\right)\right] p_{eq} - \frac{\partial}{\partial \gamma_e}(D\, p_{eq})\right) &= \\
-\frac{\partial}{\partial \gamma_e}\left(\left[\left(A - \frac{1}{\eta}\frac{\partial \Phi}{\partial \gamma_e}\right)\right] p_{eq} - \frac{\partial D}{\partial \gamma_e} p_{eq} - \frac{\partial p_{eq}}{\gamma_e} D\right) &= \\
-\frac{\partial}{\partial \gamma_e}\underbrace{\left(\left[A - \frac{\partial D}{\partial \gamma_e} + \left(\frac{D\,\Omega}{k\,T} - \frac{1}{\eta}\right)\frac{\partial \Phi}{\partial \gamma_e}\right] p_{eq}\right)}_{j} &= 0
\end{aligned}$$

The probability current j is

$$j = \left(\left[A - \frac{\partial D}{\partial \gamma_e} + \left(\frac{D\,\Omega}{k\,T} - \frac{1}{\eta}\right)\frac{\partial \Phi}{\partial \gamma_e}\right] p_{eq}\right). \tag{2.13}$$

Principal of detailed balance dictates that the probability current, j, is equal to zero for every potential Φ. Consequently one obtains

$$D = \frac{k\,T}{\Omega\,\eta}, \tag{2.14}$$

$$A = \frac{\partial D}{\partial \gamma_e}. \tag{2.15}$$

Here it is important to note that without the presence of the term A, it would be impossible for the probability current j to be zero for every potential Φ.
Inserting the expression for $\eta(\sigma)$ and then taking the derivative and assuming that $\sigma = G\gamma_e$, gives the following.

$$A(\sigma) = \frac{GkT}{\Omega\eta_0}\left(\frac{1}{\sigma}\cosh\left(\frac{\sigma}{\sigma_0}\right) - \frac{\sigma_0}{\sigma^2}\sinh\left(\frac{\sigma}{\sigma_0}\right)\right) \tag{2.16}$$

2.4 Numerical integration schemes

2.4.1 Euler-Maruyama scheme

The simplest descretization of the 1D Ito stochastic differential equation

$$\mathrm{d}X_t = f(t, X_t)\,\mathrm{d}t + g(t, X_t)\,\mathrm{d}W_t, \tag{2.17}$$

is the Euler-Maruyama scheme ,[9] p.132. For a given partition $0 = t_0 < t_1 < \ldots < t_{n-1} < t_n = t_{max}$ of the time range $\mathrm{T} = [0, t_{max}]$, the Euler-Maruyama scheme is given by

$$Y_{j+1} = Y_j + f(t_j, Y_j)(t_{j+1} - t_j) + g(t_j, Y_j)(W_{t_{j+1}} - W_{t_j}) \tag{2.18}$$

for $j = 0, 1, \ldots, n-1$, where the initial value is $Y_0 = X_0$. It is expected that the random variable Y_j generated by the iterative scheme constitutes an approximation of X_{t_j}. The quality of this approximation can be studied using the concept of the *order of strong convergence*. Suppose that $Y^{\Delta t}$ is the process generated by the iterative scheme where Δt is the maximum time step. Then it is said that the approximation scheme converges strongly with order $\nu > 0$ at time t_{max} if there exists a positive constant c, which does not depend on Δt, such that for sufficiently small Δt

$$\left\langle \left| X_{t_{max}} - Y^{\Delta t}_{t_{max}} \right|^2 \right\rangle^{\frac{1}{2}} < c(\Delta t)^{\nu}. \tag{2.19}$$

For Euler Maruyama scheme, under certain conditions the order of strong convergence $\nu = \frac{1}{2}$ can be obtained ,[9] p.132.

2.4.2 Adaptive Euler-Maruyama scheme

One of the main challenging features of simulating the stochastic Eyring model is that the time scales associated with different processes in the system are different from each other up to several orders of magnitude. In the absence of applied flow, the jumps over the energy barrier are rare events, whereas after imposing the flow these jumps become more and more frequent and near the yield point occur very fast. This implies that the time step needed to approximate the process near the yield point is much smaller than the time step needed at the beginning. In view of this discussion, one can infer that a fixed small time step algorithm during the whole simulation has either of these drawbacks:

- If it is chosen to be very small ,in order to obtain sufficient accuracy, then the running time will be very long.
- If a larger time step is chosen such that the running time becomes reasonable, then accuracy is lost.

That brings about the need for an adaptive time integration scheme. A criteria that helps choosing an appropriate time step in each iteration. The adaptive time-stepping algorithm introduced in [10] is chosen here and is as follows:

$$\begin{aligned} k_n &= G(x_n, k_{n-1}), \quad k_{-1} = K \\ x_{n+1} &= x_n + \Delta_n f(x_n) + \sqrt{\Delta_n}\, g(x_n) N(0,1) \quad x_0 = X \end{aligned}$$

where $\Delta_n = 2^{-k_n}\Delta_{max}$, and

$$\mathcal{G}(x,l) = \min\{k \in \mathrm{Z}^+ : |f(x_n + \frac{\Delta_{max}}{2^k} f(x_n)) - f(x_n)| \leq \tau \;\; \& \;\; k \geq l-1\}$$

If $K \in \mathrm{Z}^+$ then $k_n \in \mathrm{Z}^+$ and the error control enforces the condition $\Delta_n \leq \min\{2\Delta_{n-1}, \Delta_{max}\}$, where Δ_{max} is the fixed maximum time-step. In other words, for a new iteration the time step can get as small as needed by using larger values for k_n, or if unnecessary, the time step becomes bigger by setting $k_n = k_{n-1} - 1$ and checking whether $\Delta_n \leq \Delta_{max}$. In summary the algorithm can be written as follows:

$k \leftarrow 1$ ▷ $k_{-1} = K = 1$
for $i = 1 : N$ **do** ▷ Takes N time step
  if $k > 0$ **then**
    $k \leftarrow k - 1$
  end if
  while $|f(x_n + \frac{\Delta_{max}}{2^k} f(x_n)) - f(x_n)| > \tau$ **do**

$k \leftarrow k + 1$;
end while
$\mathrm{d}t \leftarrow \dfrac{\Delta_{max}}{2^k}$;
compute the solution in the next time step
end for

This algorithm converges in τ, the error control in drift term, and not in Δt converging to zero.
In order to see how this adaptive time integration scheme works, a test problem is presented. Consider the Ito SDE

$$\mathrm{d}x_t \quad = \quad (12 + 10\sin(3x_t))\mathrm{d}t + D\ \mathrm{d}W_t$$

with $x(0) = 1$. The numerical solution of this SDE using adaptive Euler-Maruyama scheme is shown in figure (2.4). One observes that the optimal time step in each iteration might change several orders of magnitude. In a non adaptive scheme, a very small time step makes the computation very long and a large time step affects the accuracy of the results. An adaptive scheme brings a balance between time efficiency and accuracy.

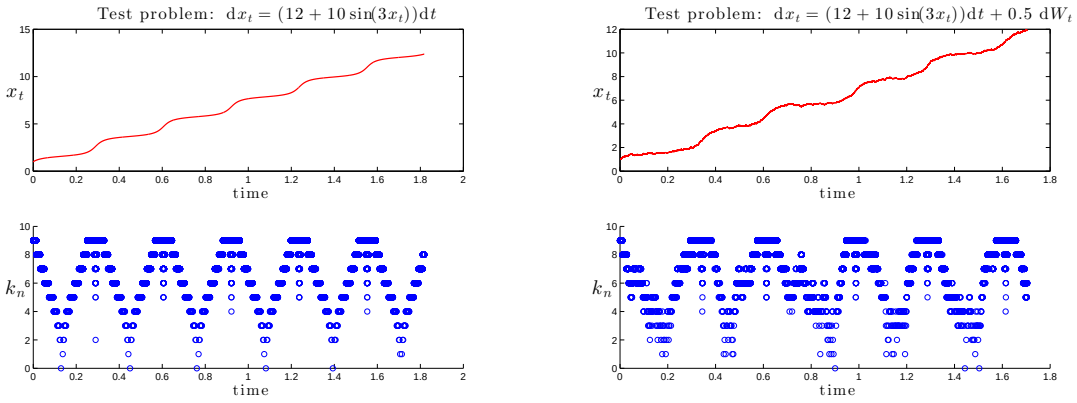

FIGURE 2.4: The red line is the numerical solution of the corresponding equation and the blue scatter plot shows values of k_n, noting that $\Delta_n = 2^{-k_n}\Delta_{max}$

2.5 Results

The adaptive time-stepping algorithm is applied to equation (2.10) to obtain Figure 2.5. As expected, for small sample volumes, near the yield point fluctuations are observed. That is due to the fact that the amplitude of the noise is inversely proportional to the sample volume as seen from equation (2.14). Moreover the scatter plot in Figure 2.5 shows that the time steps chosen by the adaptive scheme differ significantly from

each other in agreement with the previous discussion on rare and frequent jumps over the energy barrier. Now that the stochastic feature of the problem is shown, a good

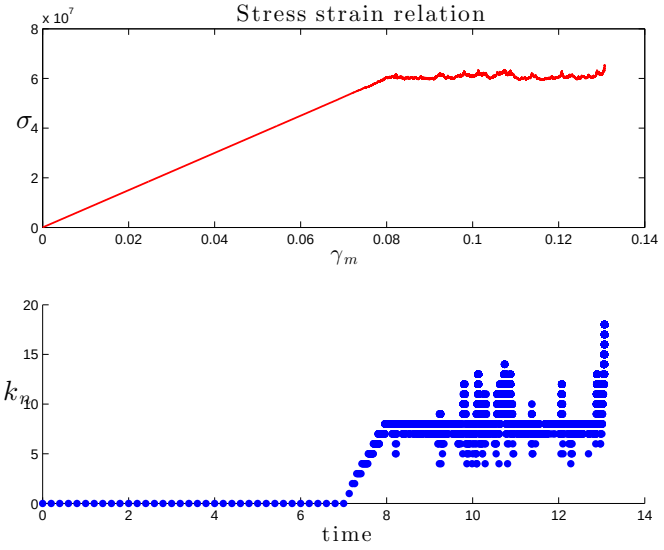

FIGURE 2.5: The top graph is simulation of a single trajectory of stress-strain curve for shear test of a sample of PC having a volume $\Omega = 10$ nm^3. Below shows how the factor k_n in adaptive algorithm is chosen in the course of time

question to ask is how the expected value of the solution looks like. The expected value of the solution can easily be obtained by taking an ensemble average of the trajectories at each time as shown in Figure 2.6. The sample volume is taken small enough so that fluctuations become observable. The mean value of the solution does not show a meaningful deviation from the deterministic model. The amplitude of the noise before reaching the yield point is not powerful enough to change the path and as a result the sharp transition to yield is not smoothed by adding noise. There are different approaches to obtain a stress-strain curve with smooth transition to yield. One approach is to consider a disorder in the parameters of the problem, in the sense that some parameters are random variables with certain distribution. This is briefly studied in appendix A.
Now that a simple SDE is not capable of capturing the actual behaviour of the system as observed in experiment, other approached need to be considered. Note that polymer chains form an entangled network, hence slipping of a chain (or a bundle of chains) might cause neighbouring chains to slip as well. This suggests constructing a model in which blocks of polymers are considered as interacting particles. This idea shall be discussed in the next chapter.

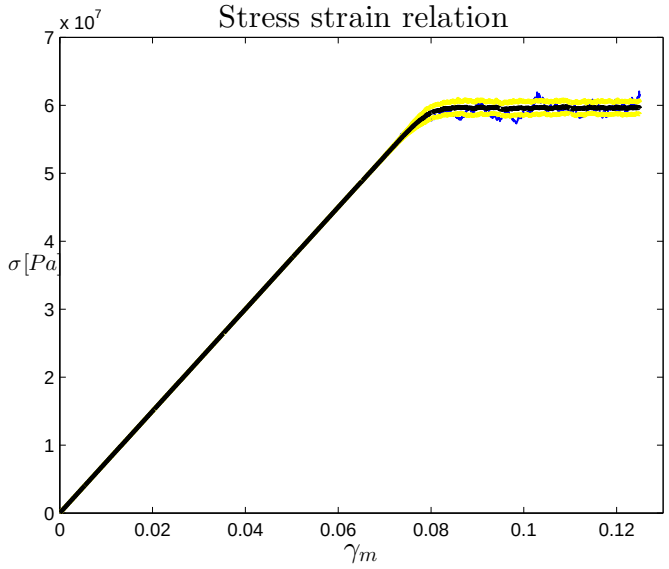

FIGURE 2.6: Ensemble average of trajectories for a sample having a volume $\Omega = 10\ \text{nm}^3$. The Black line is the average, the blue line is a single realization of a trajectory, and the two yellow lines shows the standard deviation from the mean.

Chapter 3

Particle systems approach

3.1 Particle systems approach

Polymer chains form an entangled network, hence slipping of a chain or a bundle of chains affects the neighbouring chains. This means that different parts of a polymer affect the evolution of each other in plastic flow. Having this fact in mind, the problem is revisited through a particle systems approach. Consider a one dimensional array of m polymer blocks on a circle, i.e., the mth block is attached to the first one. The whole system undergoes shear deformation with a constant strain rate. An attempt will be made to write down a vector form of the SDE (2.10) and allow mean-field effects to be present.

The evolution equation describing this particle system, inspired by equation (2.10), is proposed to have the following vector form,

$$\mathrm{d}\boldsymbol{\gamma_e} \;=\; (\dot{\boldsymbol{\gamma}}_{\boldsymbol{m}} + \boldsymbol{A} - \mathbf{M}\,\nabla_{\gamma_e}\,\Phi)\,\mathrm{d}t + \mathbf{B}\,\mathbf{dW_t} \tag{3.1}$$

where Φ is the strain energy density function of the system. Matrix $\mathbf{M}$ plays the role of the inverse viscosity in equation (2.10). Mean-field effects can be implemented in many ways. In the case the equations are decoupled, matrices $\mathbf{B}$, $\mathbf{M}$, and $\mathbf{A}$ are diagonal. Introducing off-diagonal elements in $\mathbf{B}$ or $\mathbf{M}$ can bring about mean-field effects. Another option is to consider a coupled dependence of stress on elastic strain i.e. in relation $\Phi = \frac{1}{2}\boldsymbol{\gamma_e}^T\mathbf{G}\boldsymbol{\gamma_e}$ assume that the tensor $\mathbf{G}$ has off-diagonal elements. In what follows, only one of these effects is implemented and discussed, mean-field interaction through matrix $\mathbf{B}$. According to [9],p111, the Fokker-Planck equation associated to this SDE is,

$$\frac{\partial p}{\partial t} \;=\; -\nabla_{\gamma_e}\cdot\left[\left(\dot{\boldsymbol{\gamma}}_{\boldsymbol{m}} + \boldsymbol{A} - \mathbf{M}\,\nabla_{\gamma_e}\,\Phi\right)p\right] + \nabla_{\gamma_e}\cdot\left(\nabla_{\gamma_e}\cdot(\mathbf{D}p)\right) \tag{3.2}$$

where $\mathbf{D} = \frac{1}{2}\mathbf{B}\mathbf{B}^T$.

Requiring that the equilibrium distribution is of the form $p_{eq} = Z^{-1}\exp\left(\frac{-\Phi\Omega}{kT}\right)$, one can obtain a relation between $\mathbf{A}$, $\mathbf{M}$, and $\mathbf{D}$.

$$\begin{aligned}
-\nabla_{\boldsymbol{\gamma_e}} \cdot \left[\left(\mathbf{A} - \mathbf{M}\,\nabla_{\boldsymbol{\gamma_e}}\Phi\right)p_{eq} - \nabla_{\boldsymbol{\gamma_e}} \cdot (\mathbf{D}p_{eq})\right] &= 0 \\
\left(\mathbf{A} - \mathbf{M}\,\nabla_{\boldsymbol{\gamma_e}}\Phi\right)p_{eq} - \nabla_{\boldsymbol{\gamma_e}} \cdot (\mathbf{D}p_{eq}) &= 0 \qquad \text{Principle of detailed balance} \\
\left[(\mathbf{A} - \nabla_{\boldsymbol{\gamma_e}} \cdot \mathbf{D}) + (\frac{\Omega}{kT}\mathbf{D} - \mathbf{M})\nabla_{\boldsymbol{\gamma_e}}\Phi\right]p_{eq} &= 0
\end{aligned}$$

The last equality must hold for every Φ and that means that,

$$\begin{aligned}
\mathbf{M} &= \frac{\Omega}{kT}\mathbf{D} \\
\mathbf{A} &= \nabla_{\boldsymbol{\gamma_e}} \cdot \mathbf{D}
\end{aligned}$$

3.1.1 Magnitude of the noise

For the sake of simplicity let us introduce

$$F_i := \sqrt{\frac{2kT}{\Omega\eta(\sigma_i)}}.$$

Obviously matrix $\mathbf{B}$ in the absence of mean-filed effects have a diagonal form with F_i on its diagonal. The next step would be constructing a matrix $\mathbf{B}$ that brings mean-field effects to the problem. To that end, assume that $\mathbf{B}$ has the following form

$$\mathbf{B} = \begin{pmatrix} \beta_{11} & \beta_{12} & \cdots & \beta_{1m} \\ \beta_{21} & \beta_{22} & & \\ \vdots & & \ddots & \\ \beta_{m1} & \beta_{m2} & \cdots & \beta_{mm} \end{pmatrix} \begin{pmatrix} F_1 & & & \\ & F_2 & & \\ & & \ddots & \\ & & & F_m \end{pmatrix}.$$

where β_{ij} are real numbers and serve as weights to the elements of the noise vector. In other words, the jth block affects the noise in the ith block by adding $\beta_{ij}F_j$ to the noise in the ith block.

Now the question is what are the acceptable values for β_{ij}. Suppose that at some time the stress in all blocks is the same. Then one can require that despite the presence of mean-filed effects, the evolution equation in each block be independent of the other blocks. In other words, if the stress at some time is the same in all blocks, then due to symmetry of the problem one can require that the dynamics of all block be the same. This can be achieved if they evolve independently and with the same evolution equation. To explain this point let $\boldsymbol{\beta}$ be a matrix that contains β_{ij}. Then in the case that all blocks

have equal stresses, hence equal values of F_i for $i = 1, ...m$, one can write $F_i = F$ and

$$\mathbf{B} = F\boldsymbol{\beta}$$

and introduce

$$\boldsymbol{dW'_t} := \boldsymbol{\beta} \boldsymbol{dW_t}.$$

Independence of the evolution equations requires that $< (\boldsymbol{dW'_t})_i (\boldsymbol{dW'_t})_j >= \delta_{ij}$ holds for all i and j.

$$\begin{aligned}
< (\boldsymbol{dW'_t})_i (\boldsymbol{dW'_t})_j > &= < \sum_{k=1}^{m} \beta_{ik} (\boldsymbol{dW_t})_k \sum_{l=1}^{m} \beta_{jl} (\boldsymbol{dW_t})_l > \\
&= \sum_{k=1}^{m} \sum_{l=1}^{m} \beta_{ik} \beta_{jl} < (\boldsymbol{dW_t})_k (\boldsymbol{dW_t})_l > \\
&= \sum_{k=1}^{m} \sum_{l=1}^{m} \beta_{ik} \beta_{jl} \delta_{kl} \\
&= \sum_{k=1}^{m} \beta_{ik} \beta_{jk} \\
&= \boldsymbol{\beta} \boldsymbol{\beta}^T
\end{aligned}$$

This directly implies that $\boldsymbol{\beta}$ is an orthogonal matrix since it should satisfy the following relation

$$\boldsymbol{\beta} \boldsymbol{\beta}^T = \mathbf{I} \tag{3.3}$$

Now that $\mathbf{B}$ is constructed, one can simplify $\mathbf{A}$ to get

$$\begin{aligned}
A_j &= \sum_{i=1}^{m} \frac{\partial D_{ij}}{\partial \gamma_{ei}} \\
&= \frac{1}{2} \sum_{i=1}^{m} \frac{\partial}{\partial \gamma_{ei}} \sum_{k=1}^{m} (B_{ik} B_{jk}) \\
&= \frac{1}{2} \sum_{i=1}^{m} \frac{\partial}{\partial \gamma_{ei}} \sum_{k=1}^{m} (\beta_{ik} \beta_{jk} F_k^2) \\
&= \frac{1}{2} \sum_{i=1}^{m} \sum_{k=1}^{m} (\beta_{ik} \beta_{jk}) \frac{\partial}{\partial \gamma_{ei}} (F_k^2) \\
&= \frac{1}{2} \sum_{i=1}^{m} (\beta_{ii} \beta_{ji}) \frac{\partial}{\partial \gamma_{ei}} (F_i^2) \ .
\end{aligned}$$

and for $\mathbf{M}$

$$M_{ij} = \frac{\Omega}{2kT}\sum_{k=1}^{m}(\beta_{ik}\beta_{jk}F_k^2)$$

3.2 Result and discussion

There is quite a lot of freedom in choosing the orthogonal matrix $\boldsymbol{\beta}$. Therefore a random orthogonal matrix seems to be a good starting point. Then the adaptive Euler-Maruyama algorithm that was previously discussed can be applied to the particle system and the result for different random orthogonal matrices is depicted in Figure 3.1. It is

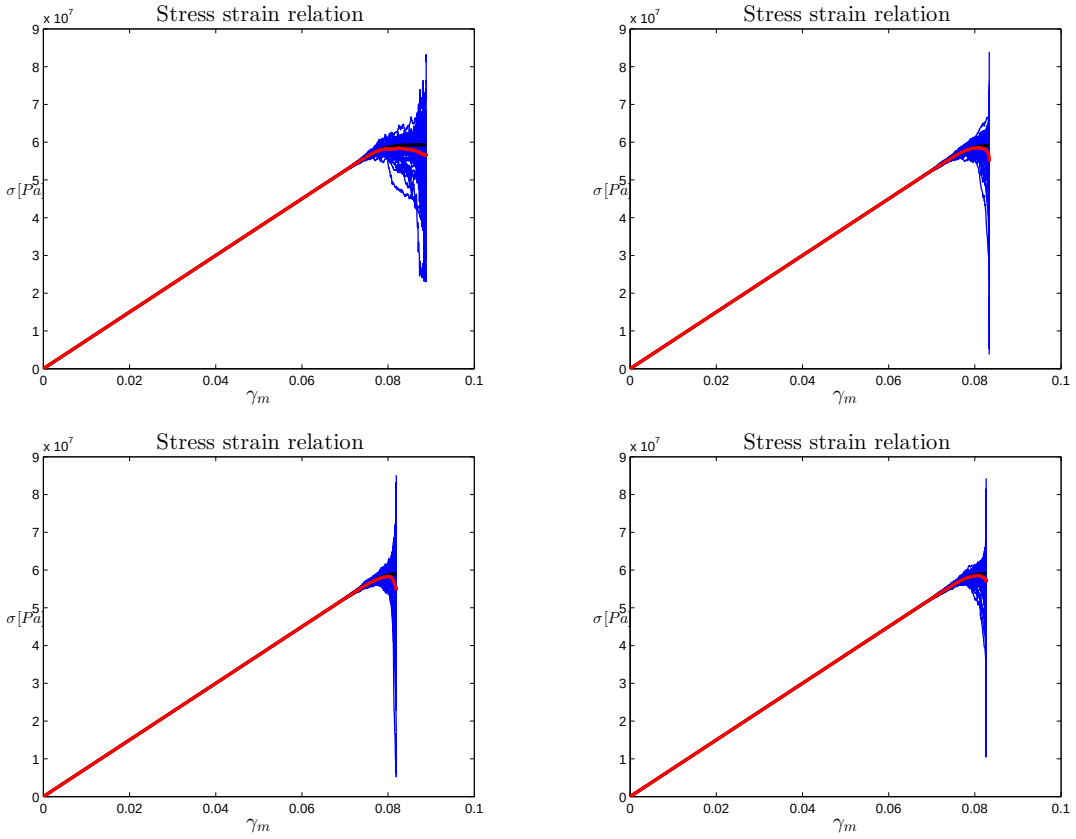

FIGURE 3.1: Results of the simulation of the particle system for different random orthogonal matrices. The ensemble average in red, individual trajectories in blue and the deterministic solution in black

seen that the transition to yield is still a sharp kink and the path follows the deterministic solution. More important is the behaviour of the (average) solution after the yield point. A softening behaviour is observed which fits very well with post-yield behaviour of polymers observed in experiments, see Figure 2.3. Therefore from an engineering point of view it might be interesting to see that this particle systems approach with mean-field interactions produces softening. It is important to note that this softening

behaviour is observed no matter what orthogonal matrix $\boldsymbol{\beta}$ is chosen. There are many ways to generate orthogonal matrices which are not discussed here.

A closer look at individual trajectories in Figure 3.1 shows that some of them continue to go down after the yield point in such a way that seems not to be compatible with the physics of the problem. One does not expect the stress in a polymer block to become almost zero after the yield point. This behaviour which can be regarded as a kind of destabilization, is mainly due to large fluctuations of the noise.

At this point one can doubt whether an SDE description of Eyring model is valid in large amplitude noise regime. This brings about the need for a more rigorous understanding of the stochastic process describing plastic flow and see in what situations this stochastic process can be expressed in terms of a stochastic differential equation and the corresponding Fokker-Planck equation. In the next chapter a new model is developed to see more rigorously how right is a the stochastic description provided until now.

Chapter 4

A Discrete Model

4.1 Random walk as a model for polymer plasticity

The aim of this chapter is to construct another model for plastic deformation of polymers based on a discrete stochastic process. As a motivation, before going into details of the model, it is important that the molecular mechanism of deformation be made more clear. The stiffness of polymers is due to the strength of the bonds involved: inter-molecular and intra-molecular. The bonds that hold together a single chain are too strong to break and they contribute to the elastic component of deformation. The bonds between different polymer chains are weaker and their breakage allow slippage and stretching, consequently they contribute to the viscous part of the deformation process [11]. The viscous part of the deformation is a thermally activated process and using this fact a new model is constructed as follows.

Consider a 1d regular lattice and a particle that moves on this lattice with certain forward and backward jump rates. Suppose that this particle is attached to one end of a spring and the other end of the spring moves with a fixed speed v, as shown in Figure 4.1. The movement of the side of the spring with speed v is followed by elastic change

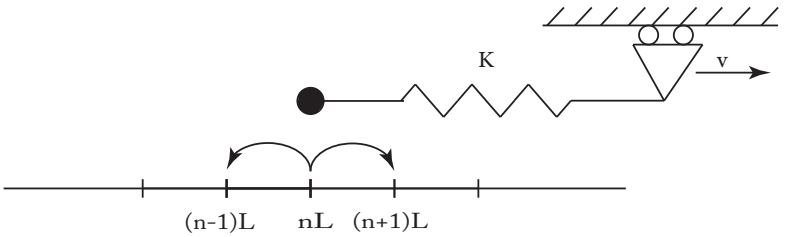

FIGURE 4.1: Discrete model for plastic deformation

of the length of the spring and the movement of the particle on the lattice. If the movement of the particle is such a way that resembles the jumps over the energy barrier in

Eyring model, then this system can perfectly describe a discrete version of the plastic deformation process as will be shown.
Assume that the forward and backward jump rates are given by a Kramer-type expression.

$$r_f(t) = \alpha_L \exp\left(+\frac{f(t)L^*}{kT}\right) \tag{4.1}$$

$$r_b(t) = \alpha_L \exp\left(-\frac{f(t)L^*}{kT}\right) \tag{4.2}$$

where L is the distance between sites in the regular lattice, f is the force in the spring, and L^* is a fixed length inspired by the activation volume in Eyring model. The prefactor α_L is

$$\begin{aligned} \alpha_L &= \frac{\alpha_0}{L^\lambda} \exp\left(-\frac{\Delta E}{kT}\right) \\ &= \frac{\alpha}{L^\lambda} \end{aligned} \tag{4.3}$$

where ΔE is the height of the energy barrier between successive sites of the lattice in the absence of force field, and λ is a positive integer, yet unspecified, that scales the jump rates so that in the limit $L \to 0$ the terms in the limit equation do not vanish.
Now let $x(t)$ be the position of the particle at time t. The relation

$$x(t) = Ln(t) \tag{4.4}$$

means that if at time t the particle is at site n, then the position of the particle on the x-axis is equal to Ln. Then the change in the length of the spring is

$$u(t) = vt - x(t) \tag{4.5}$$

and consequently the force in the spring is $f(t) = Ku(t)$.
From the expressions assumed for the jump rates, one can heuristically say that the average speed of the particle is given by

$$\begin{aligned} \dot{x}(t) &\approx L(r_f - r_b) \\ &= 2L\alpha_L \sinh\left(\frac{f(t)L^*}{kT}\right). \end{aligned}$$

Hence the corresponding evolution equation describing the expected behaviour of the particle can be approximated to be

$$\dot{u} = v - 2L\alpha_L \sinh\left(\frac{f(t)L^*}{kT}\right). \tag{4.6}$$

Now for if α_L a hyperbolic scaling is chosen i.e. $\lambda = 1$, the above equation turns into the following

$$\dot{u} = v - 2\alpha \sinh\left(\frac{f(t)L^*}{kT}\right) \tag{4.7}$$

which is independent of L, very much analogous to pure drift processes resulting from hyperbolic scaling, see appendix B. Clearly this equation is similar to the Eyring model for plastic deformation of polymers. In what follows, λ is not specified in order to find the proper scale for the jump rates in the limit $L \to 0$.

4.2 Nondimensionalization

Let us introduce dimensionless variables (with tilde) using yet unspecified length scales U and X and a time scale $\mathcal{T}$.

$$\begin{aligned} u &= U\tilde{u} \\ t &= \mathcal{T}\tilde{t} \\ x &= X\tilde{x} \end{aligned}$$

Equation (4.6) can be rearranged to obtain

$$\frac{d\tilde{u}}{d\tilde{t}} = \frac{\mathcal{T}v}{U} - \frac{2\mathcal{T}L\alpha_L}{U} \sinh\left(\frac{KL^*U}{kT}\tilde{u}\right) \tag{4.8}$$

In order to scale the equation as well as making it dimensionless, one can firstly find the steady state value of the solution of equation (4.6)

$$u_Y = \frac{kT}{KL^*} \sinh^{-1}\left(\frac{v}{2L\alpha_L}\right) \tag{4.9}$$

and then take $X = U = u_Y$ and $\mathcal{T} = u_Y/v$. Then equation (4.8) simplifies as follows

$$\frac{d\tilde{u}}{d\tilde{t}} = 1 - \frac{\sinh(\mu\tilde{u})}{\sinh(\mu)} \tag{4.10}$$

where $\mu = \sinh^{-1}\left(\frac{v}{2L\alpha_L}\right)$. It is seen that $\tilde{u}$ lies between 0 and 1 as intended.
Inspired by these steps, it is possible to rewrite the discrete system in a dimensionless form. By introducing $\beta = \frac{KLL^*}{kT}$ one can show that the change in the length of the spring in dimensionless form is

$$\tilde{u} = \tilde{t} - \frac{\beta}{\mu}n. \tag{4.11}$$

Here $\frac{\beta}{\mu}$ is the distance between lattice sites in dimensionless form and it is good to note that for $\lambda < 2$ one can show that

$$\lim_{L\to 0} \frac{\beta}{\mu} = 0 \tag{4.12}$$

The dimensionless form of the jump rates can be obtained by multiplying them by the time scale of the problem.

$$\begin{aligned} R_f &= \tau r_f \\ &= \frac{\alpha u_Y}{v} \exp\left(\frac{KL}{kT} u\right) \\ &= \frac{\mu}{2\beta \sinh(\mu)} \exp(\mu \tilde{u}) \end{aligned} \tag{4.13}$$

and analogously

$$R_b = \frac{\mu}{2\beta \sinh(\mu)} \exp(-\mu \tilde{u}). \tag{4.14}$$

An important observation here is that $\beta = \frac{KLL^*}{kT}$ is a dimensionless group that does not appear in the approximate equation (4.10).

4.3 Numerical simulation of the discrete model

There are different methods for simulating continuous time random walks. Two of these methods, the *fixed time method* and the *waiting time method* will be explained here briefly and then it is discussed why these two methods should be combined to form an adaptive scheme. An important feature of continuous time random walks as a Markov process is that the waiting time between successive jumps is an exponential random variable. This is a direct consequence of the Markov property of the process. More precisely, the Markov property implies that the waiting time between successive jumps is a memoryless random variable and the unique memory less random variable is generated by exponential distribution.

- **Waiting time method**
  In this method, first the waiting time until the next jump should be calculated. This waiting time is an exponentially distributed random variable with rate parameter $R_f + R_b$. After generating this waiting time, then the decision on whether

jumping to right or left is made based on the following jump probabilities.

$$p_f = \frac{R_f}{R_f + R_b} \tag{4.15}$$

$$p_b = \frac{R_b}{R_f + R_b} \tag{4.16}$$

- **Fixed time method**
  This method is suitable the most for processes whose rates are constant. The procedure is that a time interval, Δt is fixed and then the probability of jumping forward is supposed to be $p_f = R_f \Delta t$, the probability of jumping backward $p_b = R_b \Delta t$, and the probability of staying in the current position $p_s = 1 - (p_f + p_s)$. In every iteration the decision is based on these three probabilities. Note that the time step should be chosen such that the probabilities do not exceed 1.

The final aim of doing numerical simulation on this discrete system is to see the behaviour of the solution in the regime that polymers evolve in plastic flow. One of the main challenges of simulating this discrete system in that regime is that at the beginning of the process the jumps are very rare and the waiting time until the first jump is extremely large. It is not possible to wait this long period of time because the rates of the process are time dependent and before this long waiting time ends the particle has already jumped with a high probability to other sites. In other words, the waiting time in the first iteration is so large that it exceeds the total time the system needs to reach the plateau value. Therefore it is not possible to use the waiting time method.
The fixed time method also has its own problem. In the course of iteration, the jump rates increase exponentially and these rates multiplied by the fixed time step will eventually exceed 1. One can prevent this by choosing a sufficiently small fixed time step, however in that case the simulations becomes very long.
The adaptive algorithm to overcome these problems is very simple. A fixed time step is assigned and in every iteration this time step is compared to the waiting time until the next jump. If the waiting time is larger, then the process will evolve this tiny time step according to the fixed time method and if not according to the waiting time method. Then in the next iteration again the rates are calculated and the next waiting time is again compared to the assigned fixed time step and so on. It can be inferred that at the beginning of the process where the drift is dominant, the fixed time step is chosen and near reaching the plateau value where the jumps become frequent, the waiting time is chosen in the algorithm.

4.3.1 Results

Simulation of the system has two important results. One is that the sharpness of the transition to the plateau is determined only by parameter μ. The other result is that for a given μ, the magnitude of the noise can be independently tuned by β. Figure (4.2) shows a simulation result for given parameters.

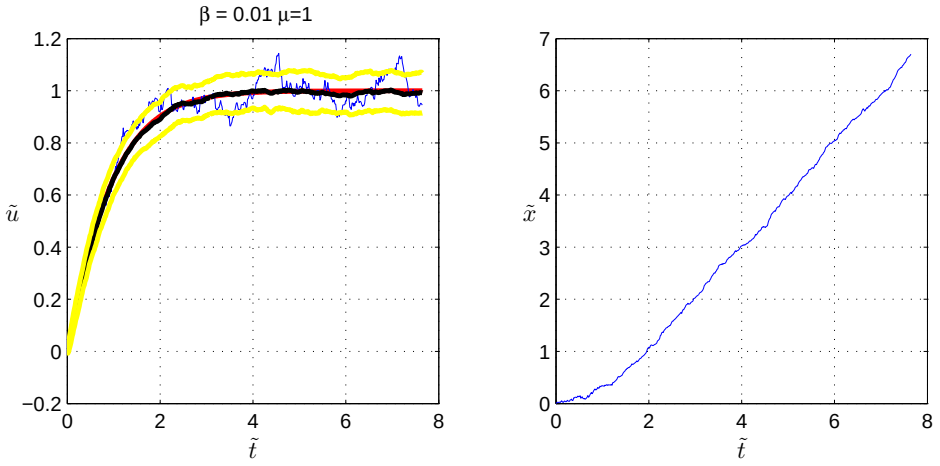

FIGURE 4.2: Solution of the discrete system for $\mu = 1$ and $\beta = 0.01$. The black line is the ensemble average of many trajectories, the red line is the solution of the heuristic averaged ODE, the blue line is a single trajectory and the two yellow lines are the standard deviation from the mean.

The ratio of $\frac{\sigma}{\sigma_0}$ in the Eyring model for polycarbonate goes from 0 to 43. Therefore by taking $\mu = 43$ it is possible to simulate the discrete system in the same regime as polycarbonate undergoes shear deformation.

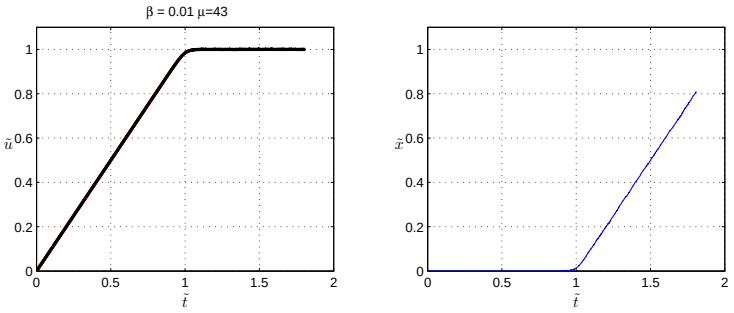

FIGURE 4.3: $\mu = 43$ and $\beta = 0.01$

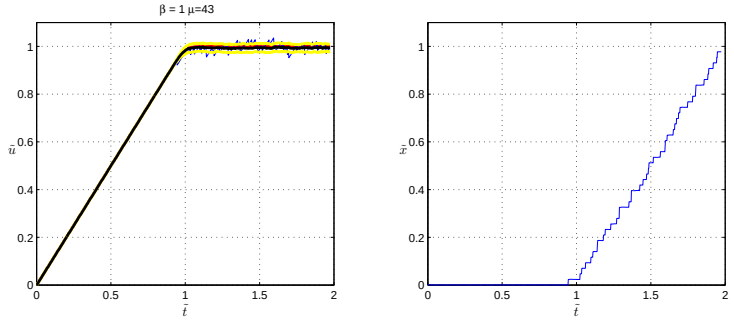

FIGURE 4.4: $\mu = 43$ and $\beta = 1$

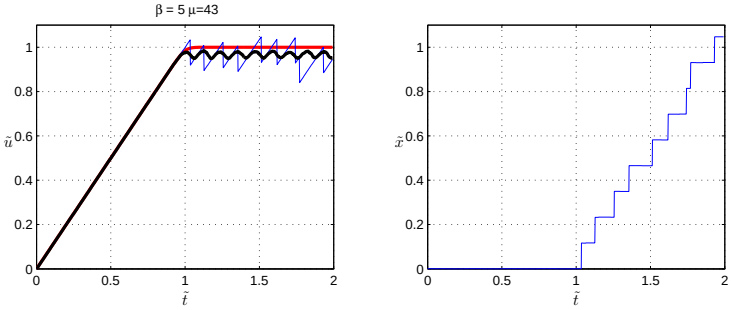

FIGURE 4.5: $\mu = 43$ and $\beta = 5$

4.4 Continuum limit of the discrete model

The results of numerical solution of the discrete systems suggest that the continuum limit can be an SDE. This SDE can be derived by finding the corresponding Fokker-Planck equation via *Kramers-Moyal expansion*.

4.4.1 Kramers-Moyal expansion

The starting point in Kramers-Moyal expansion is defining the *jump moments* [12]. For a stochastic process that is continuous in time and state space this definition is as follows

$$M_l(x,t,\Delta t) = \int (\zeta - x)^l P(\zeta, t+\Delta t|x,t) d\zeta \ . \tag{4.17}$$

Analogously for a stochastic process with discrete state space the jump moments are

$$M_l(n,t,\Delta t) = \sum_{n'} (n'-n)^l P(n', t+\Delta t|n,t). \tag{4.18}$$

Kramers-Moyal expansion says that provided that the initial conditions are known, the conditional probability $P(x, t+\Delta t|x_0,t_0)$ is

$$P(x,t+\Delta t|x_0,t_0) = \sum_{l=0}^{\infty} \frac{(-1)^l}{l!} \frac{\partial^l}{\partial x^l} \left[M_l(x,t,\Delta t) P(x,t|x_0,t_0)\right]. \tag{4.19}$$

One might drop the initial condition since they are known and does not play a role here. Further assumption is needed on the jump moments to obtain a Fokker-Planck equation. Assume that for $l \geq 1$

$$M_l(x,t,\Delta t) = D^l(x,t)\Delta t + o(\Delta t). \tag{4.20}$$

Substituting this in equation (4.19) and taking the limit $\Delta t \to 0$ gives

$$\frac{\partial P}{\partial t} = \sum_{l=1}^{\infty} \frac{(-1)^l}{l!} \frac{\partial^l}{\partial x^l} \left[D^l(x,t) P(x,t) \right]. \tag{4.21}$$

Under suitable scaling one might neglect the terms with $l > 2$ and obtain a Fokker-Planck equation.

$$\frac{\partial P}{\partial t} = -\frac{\partial}{\partial x}[D^1(x,t)P(x,t)] + \frac{1}{2}\frac{\partial^2}{\partial x^2}[D^2(x,t)P(x,t)]. \tag{4.22}$$

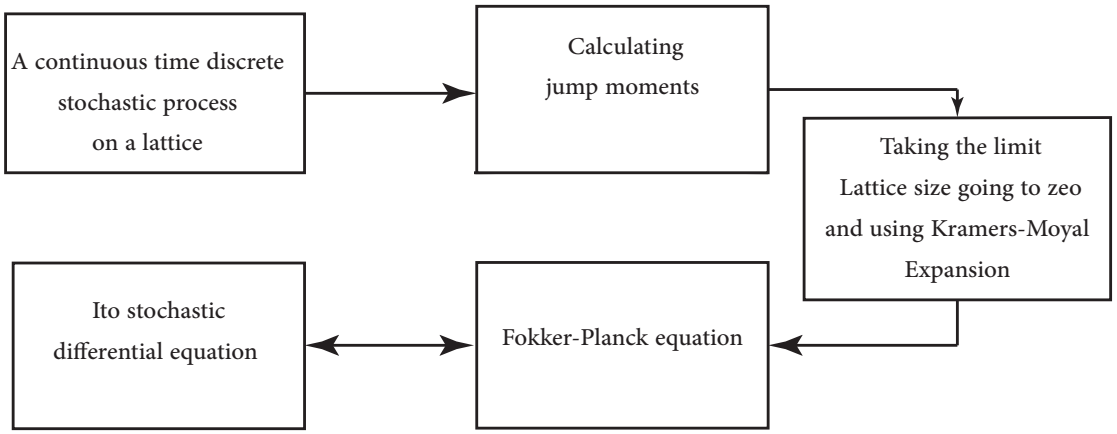

FIGURE 4.6: Procedure of taking continuum limit of a continuous time descrite Markov chain.

4.4.2 The limit of the discrete system

The first step is to calculate the jump moments for the discrete system. Using equation (4.18) and assuming that for small $\Delta\tilde{t}$ the probability of jumping more that one site is

negligible, one obtains

$$\begin{aligned} M_l(n,\tilde{t},\Delta\tilde{t}) &= \sum_{n'}(n'-n)^l P(n',\tilde{t}+\Delta\tilde{t}|n,\tilde{t}) \\ &= P(n+1,\tilde{t}+\Delta\tilde{t}|n,\tilde{t}) \\ &+ (-1)^l P(n-1,\tilde{t}+\Delta\tilde{t}|n,\tilde{t}) \\ &= R_f(n,\tilde{t})\Delta\tilde{t} + (-1)^l R_b(n,\tilde{t})\Delta\tilde{t}. \end{aligned} \tag{4.23}$$

On the other hand in the limit of the lattice size going to zero, it is obtained that

$$M_l(\tilde{x},\tilde{t},\Delta\tilde{t}) = \left(\frac{\beta}{\mu}\right)^l M_l(n,\tilde{t},\Delta\tilde{t}) \tag{4.24}$$

more precisely

$$M_l(\tilde{x},\tilde{t},\Delta\tilde{t}) = \begin{cases} \left(\frac{\beta}{\mu}\right)^{l-1} \frac{\sinh(\mu\tilde{u})}{\sinh(\mu)}\Delta\tilde{t} & \text{if } l \text{ odd}, \\ \left(\frac{\beta}{\mu}\right)^{l-1} \frac{\cosh(\mu\tilde{u})}{\sinh(\mu)}\Delta\tilde{t} & \text{if } l \text{ even} \end{cases} \tag{4.25}$$

Now the Kramers-Moyal expansion for $P(\tilde{x},\tilde{t})$ becomes

$$\begin{aligned} \frac{\partial P(\tilde{x},\tilde{t})}{\partial\tilde{t}} = &- \frac{\partial}{\partial\tilde{x}}\left[\left(\frac{\sinh(\mu\tilde{u})}{\sinh(\mu)}\right)P(\tilde{x},\tilde{t})\right] \\ &+ \frac{1}{2}\frac{\partial^2}{\partial\tilde{x}^2}\left[\left(\frac{\beta}{\mu}\frac{\cosh(\mu\tilde{u})}{\sinh(\mu)}\right)P(\tilde{x},\tilde{t})\right] + o\left(\left(\frac{\beta}{\mu}\right)^2\right) \end{aligned} \tag{4.26}$$

and since $\tilde{u} = \tilde{t} - \tilde{x}$, after neglecting the terms with $l > 2$ it follows that

$$\frac{\partial P(\tilde{u},\tilde{t})}{\partial\tilde{t}} = -\frac{\partial}{\partial\tilde{u}}\left[\left(1 - \frac{\sinh(\mu\tilde{u})}{\sinh(\mu)}\right)P(\tilde{u},\tilde{t})\right] + \frac{1}{2}\frac{\partial^2}{\partial\tilde{u}^2}\left[\left(\frac{\beta}{\mu}\frac{\cosh(\mu\tilde{u})}{\sinh(\mu)}\right)P(\tilde{u},\tilde{t})\right] \tag{4.27}$$

To make the procedure of taking the limit $L \to 0$ more clear, equation (4.27) is transformed into its dimensional form for evolution of u.

$$\begin{aligned} \frac{\partial P(u,t)}{\partial t} = &- \frac{\partial}{\partial u}\left[\left(v - 2L\alpha_L \sinh\left(\frac{KuL^*}{kT}\right)\right)P(u,t)\right] \\ &+ \frac{1}{2}\frac{\partial^2}{\partial u^2}\left[\left(2L^2\alpha_L \cosh\left(\frac{KuL^*}{kT}\right)\right)P(u,t)\right] \end{aligned} \tag{4.28}$$

The question here is how should α_L scale with L, or what value should λ take in view of equation (4.3), in order for Kramers-Moyal Expansion to be a good approximation. Inspired by the classical example of biased diffusion on a lattice discussed in appendix B, here $\lambda = 1$ seems to be appropriate, i.e. the rates scale with $1/L$. This choice will result in a drift term which is independent of L and a diffusion term that is of order one

in L. The next terms are of higher order in L and can be truncated. Now it is possible to obtain a stochastic differential equation for $\tilde{u}$ using equation (4.27).

$$d\tilde{u} = \left(1 - \frac{\sinh(\mu\tilde{u})}{\sinh(\mu)}\right) d\tilde{t} + \sqrt{\frac{\beta}{\mu}\frac{\cosh(\mu\tilde{u})}{\sinh(\mu)}} dW_{\tilde{t}} \tag{4.29}$$

and in dimensional form

$$du = \left(v - 2\alpha \sinh\left(\frac{KuL^*}{kT}\right)\right) dt + \sqrt{2L\alpha \cosh\left(\frac{KuL^*}{kT}\right)} dW_t \tag{4.30}$$

4.5 Discussion

Let us rewrite the two Fokker-Planck equations obtained as a model for plastic deformation.
The limit of the discrete model:

$$\begin{aligned}\frac{\partial P(u,t)}{\partial t} = &- \frac{\partial}{\partial u}\left(\left[v - 2\alpha_0 \exp(-\frac{\Delta E}{kT}) \sinh\left(\frac{KuL^*}{kT}\right)\right] P(u,t)\right) \\ &+ \frac{\partial^2}{\partial u^2}\left(\left[L\alpha_0 \exp(-\frac{\Delta E}{kT}) \cosh\left(\frac{KuL^*}{kT}\right)\right] P(u,t)\right).\end{aligned}$$

and the stochastic Eyring model from chapter 2

$$\begin{aligned}\frac{\partial p(\gamma_e,t)}{\partial t} = &- \frac{\partial}{\partial \gamma_e}\left(\left[\dot{\gamma}_m + A(\sigma) - \dot{\gamma}_0 \exp(-\frac{\Delta E}{kT}) \sinh(\frac{\sigma}{\sigma_0})\right] p(\gamma_e,t)\right) \\ &+ \frac{\partial^2}{\partial \gamma_e^2}\left(\left[\frac{kT}{\Omega}\dot{\gamma}_0 \exp(-\frac{\Delta E}{kT})\frac{1}{\sigma}\sinh\left(\frac{\sigma}{\sigma_0}\right)\right] p(\gamma_e,t)\right)\end{aligned}$$

The drift term in the first equation is exactly the heuristic averaged equation (4.6). This means that the SDE describing the system is just the averaged ODE with a noise term added. Moreover, it justifies the approach in chapter 2 that a noise was added to the Eyring model to obtain a stochastic version.
During plastic flow, individual flow units affect the deformation process by a certain amount. The size of these contributions relative to the volume of the sample under shear determines the size of fluctuations of stress-strain curve. The lattice size L is a representative of this relative size This means that the smaller the sample volume is, the larger is the relative distance L and vice versa. In other words L is inversely proportional to the sample volume. It was seen the amplitude of the noise in the stochastic Eyring model scales with $\sqrt{\frac{1}{\Omega}}$ and in the limit of the discrete system with $\sqrt{L}$. In this sense the two models are in harmony with each other.

As mentioned before, the limit equation (4.27) is valid for sufficiently small L, or equivalently saying, for sufficiently large sample volumes. This means that when the sample volume is very small and the system is in the large fluctuations regime, then describing the system with stochastic differential equation and associated Fokker-Planck equation is under question.

Chapter 5

Conclusion and future work

5.1 Conclusion

This thesis deals with concepts in mechanics and thermodynamics of materials, mainly polymers, during plastic flow and in this respect various mathematical tools are used. Results and techniques in stochastic calculus, discrete stochastic processes, time integration techniques for SDEs are extensively utilized.

Polymer chains contribute to plastic deformation by breaking (inter-molecular) bonds and slipping on each other. This process is of statistical nature and brings the need to describe the system with a stochastic differential equation. In chapter 2 an SDE is derived based on the assumption that in equilibrium i.e. in the absence of applied flow, elastic deformation obeys a Boltzmann distribution. Then it was seen that the magnitude of the noise is inversely proportional to the sample volume, however the expected value of the solution of the SDE does not differ much from the deterministic ODE.

In the next step, chapter 3, an attempt was made to show how one can construct an interacting particle system out of polymer blocks under shear. Then one possible approach was implemented and the results turn out to be controversial. Softening in the post-yield behaviour is observed in simulations, however destabilization of individual trajectories brings about doubt in equivalence of SDE and the corresponding Fokker-Planck equation.

In chapter 4, a whole new model is developed. This new toy model is a discrete representative of the random events behind plastic strain rate. The continuum limit of this discrete system is taken via Kramers-Moyal expansion. The resulting Fokker-Planck equation is shown to be valid only is small amplitude noise regime. Moreover a connection between this model and the model in chapter 2 is established.

5.2 Recommendation for future work

Future work in the direction of this thesis would mainly consist of working on the interacting particle system and introducing different mean-field effects. It is very important to note that describing the system with SDE and the associated Fokker-Plack equation is valid only in small amplitude noise regime. Therefore it is better to do direct simulation of the discrete model as an interacting particle system.
Also it would be very interesting to study the time correlation of the fluctuations of the discrete system and see if it is possible to make a connection with plastic strain rate.
It seems very crucial to perform a detailed molecular dynamics simulation of polymers during plastic deformation and hope that the result can shed light on the various phenomena at molecular level.

Bibliography

[1] E.T.J. Klompen Mechanical properties of solid polymers: constitutive modelling of long and short term behaviour. *Ph.D. Thesis. Eindhoven University of Technology: The Netherlands*, 2005.

[2] H. Eyring A. S. Krausz. Deformation Kinetics, wiley-interscience, new york, 1975, 398 pp.

[3] JR White. On internal stress and activation volume in polymers. *Journal of Materials Science*, 16(12):3249–3262, 1981.

[4] H. Eyring. Viscosity, plasticity, and diffusion as examples of absolute reaction rates. *The Journal of Chemical Physics*, 4:283, 1936.

[5] I. M. Ward and D.W. Hadley. *An introduction to the mechanical properties of solid polymers.* John Wiley & Sons Ltd.; John Wiley & Sons, Inc., 1993.

[6] L.C.A. Van Breemen, E.T.J. Klompen, L.E. Govaert, and H.E.H Meijer. Extending the egp constitutive model for polymer glasses to multiple relaxation times. *Journal of the Mechanics and Physics of Solids*, 59(10):2191–2207, 2011.

[7] Kan Cao, Xinzhong Ma, Baoshan Zhang, Yang Wang, and Yu Wang. Tensile behavior of polycarbonate over a wide range of strain rates. *Materials Science and Engineering: A*, 527(16):4056–4061, 2010.

[8] M. Hütter, M. Grmela, and H. C. Öttinger. What is behind the plastic strain rate? *Rheologica acta*, 48(7):769–778, 2009.

[9] H. C. Öttinger. *Stochastic processes in polymeric fluids: tools and examples for developing simulation algorithms.* Springer Berlin, 1996.

[10] H Lamba, Jonathan C Mattingly, and Andrew M Stuart. An adaptive euler–maruyama scheme for sdes: convergence and stability. *IMA Journal of Numerical Analysis*, 27(3):479–506, 2007.

[11] Alexander Stephen Krausz and Henry Eyring. *Deformation kinetics*, volume 197. Wiley New York, 1975.

[12] A.J. McKane. *Stochastic Processes in Encyclopedia of Complexity and System Science*. Springer, 2009.

Quenched Disorder

Quenched disorder is a constrained disorder in a system that evolves in time. In statistical physics, when some parameters of a system are randomly distributed and unchanged in time, it is said that the system is showing quenched disorder.
In the problem of plastic deformation of polymers there are certain parameters that are assumed to have a fixed value, like the shear modulus G or the height of the energy barrier ΔE. However, the glassy nature of many polymers, in particular polycarbonate, suggests the use of quenched disorder in the parameters of the problem. One can construct a non-interacting particle system in which one or more parameters are randomly distributed. Here a normal distribution is used to obtain Figures (1) and (2). It is observed that indeed quenched disorder makes the stress-strain curve show a smooth transition to yield.

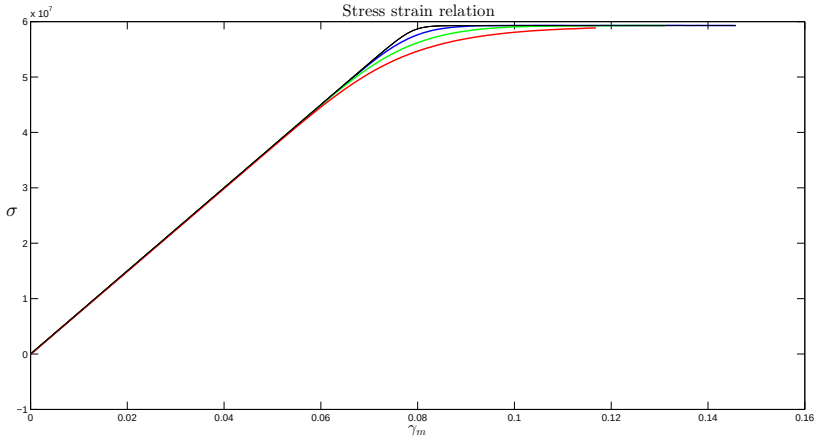

FIGURE 1: Solution using quenched disorder for the shear Modulus G. Normal distribution for G with mean value 750 MPa and standard deviation 50MPa (blue), 100MPa(green), and 150MPa(red). The black line is the deterministic solution

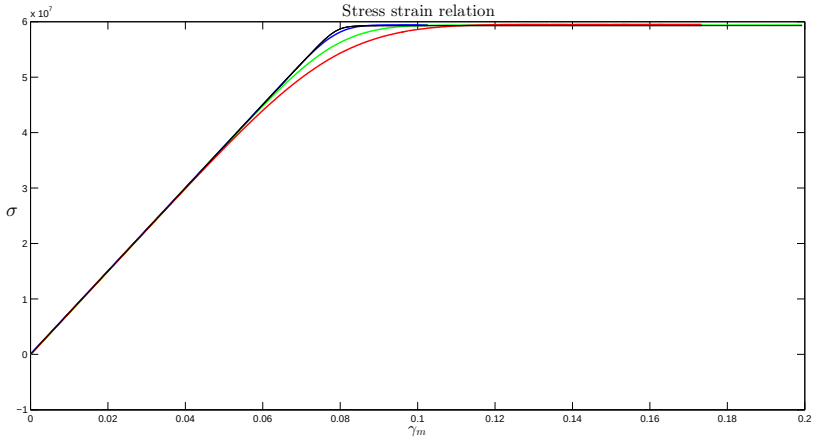

FIGURE 2: Solution using quenched disorder for the activation energy ΔE. Normal distribution for ΔE with mean value 274 KJ and standard deviation 5 KJ (blue), 15 KJ(green), and 25 KJ(red). The black line is the deterministic solution

Biased diffusion

. Consider a particle jumping on a regular lattice with constant rates.

$$\begin{aligned} r_f &= \frac{p}{\tau_L} \\ r_b &= \frac{(1-p)}{\tau_L} \end{aligned}$$

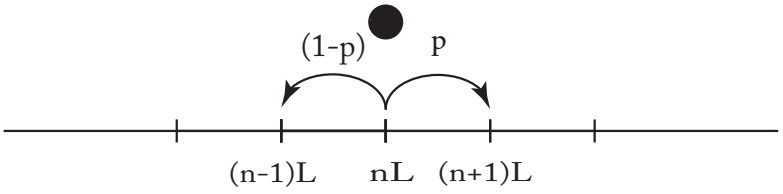

FIGURE 3: Biased diffusion on a regular lattice

In order to obtain the continuum limit of this continuous time random walk, first the jump moments should be obtained. Analogous to the discussion in chapter 4 it is easy to see that

$$\begin{aligned} M_l(n,t,\Delta t) &= \sum_{n'}(n'-n)^l P(n',t+\Delta t|n,t) \\ &= r_f\Delta t + (-1)^l r_b \Delta t. \end{aligned}$$

The continuous version is obtained by considering $x = nL$:

$$M_l(x,t,\Delta t) = \begin{cases} \dfrac{(2p-1)}{\tau_L} L^l \Delta t & \text{if } l \text{ odd}, \\ \\ \left(\dfrac{1}{\tau_L}\right) L^l \Delta t & \text{if } l \text{ even} \end{cases} \tag{1}$$

Then the Kramers-Moyal expansion follows to be

$$\frac{\partial P(x,t)}{\partial t} = -\frac{\partial}{\partial x}\left((2p-1)\frac{L}{\tau_L}P(x,t)\right) + \frac{1}{2}\left(\frac{L^2}{\tau_L}P(x,t)\right) + O(\frac{L^3}{\tau_L}) \tag{2}$$

Now it should be made clear what happens in the limit $L \to 0$. In order not to kick out all the terms, one needs to rescale the jump rates. There are two possibilities:

- **Parabolic scaling**, $\tau_L = L^2\tau_0$
  This scaling for the case of symmetric random walk i.e. $p = \frac{1}{2}$ results in a diffusion equation independent of L, with diffusion coefficient $D = \frac{1}{2\tau_0}$. But for the biased random walk, results in a drift term that tends to infinity as $L \to 0$. Therefore parabolic scaling is not a good choice for drift dominant processes.

- **Hyperbolic scaling**, $\tau_L = L\tau_0$
  By this scaling the drift term becomes independent of L with speed $v = \dfrac{(2p-1)}{\tau_0}$. However the diffusion term is now of order one is L and hence vanishes in the Limit $L \to 0$. One way to deal with this issue is to keep the diffusion term and kick the terms who are of order larger that one. In this way, for any L we have a Fokker-Planck equation as a coarse-grained description of the discrete stochastic process. The smaller L is the better the Fokker-Planck equation approximates the discrete system.